BCSJ

Synthesis and Photophysical Properties of Eu(III) Complexes with Phosphine Oxide Ligands including Metal Ions

Masanori Yamamoto,[1] Takayuki Nakanishi,[2] Yuichi Kitagawa,[2] Tomohiro Seki,[2] Hajime Ito,[2] Koji Fushimi,[2] and Yasuchika Hasegawa*[2]

[1]Graduate School of Chemical Sciences and Engineering, Hokkaido University, Kita 13-Jo, Nishi 8-Chome, Kita-ku, Sapporo, Hokkaido, 060-8628

[2]Faculty of Engineering, Hokkaido University, Kita-13 Jo, Nishi-8 Chome, Kita-ku, Sapporo, Hokkaido, 060-8628

E-mail: hasegaway@eng.hokudai.ac.jp

Received: July 26, 2017; Accepted: September 22, 2017; Web Released: October 12, 2017

Abstract

Lanthanide (Ln^{3+}) complexes composed of luminescent Eu^{3+} complex and joint metal blocks (Al^{3+}, Zn^{2+} and Pd^{2+} complexes) are reported. The Eu^{3+} complexes $[Eu(hfa)_3(dppy)_2PdCl_2]_n$ (Eu-Pd), $[Eu(hfa)_3(dppy)_2ZnCl_2]_n$ (Eu-Zn) and $[Eu(hfa)_3(dppy)_4AlCl_3]_n$ (Eu-Al) (hfa: hexafluoroacetylacetonato, dppy: 4-pyridyldiphenylphosphine oxide) were synthesized by the complexation of $[Eu(hfa)_3(H_2O)_2]$ with $[MCl_n(dppy)_m]$ ($M = Pd^{2+}$, Zn^{2+} and Al^{3+}). These predicted structures were estimated using single-crystal X-ray structural analyses and DFT calculations. Photophysical properties of these complexes were evaluated based on the emission lifetimes and emission quantum yields. The emission quantum yields are dependent on the moiety of the joint metal blocks. Eu-Al complex shows the largest emission quantum yield ($\Phi_{ff} = 72\%$). In contrast, the emission quantum yield of Eu-Pd is found to be 1.3%. The structures and photophysical properties of Eu^{3+} complexes linked with joint metal blocks are demonstrated.

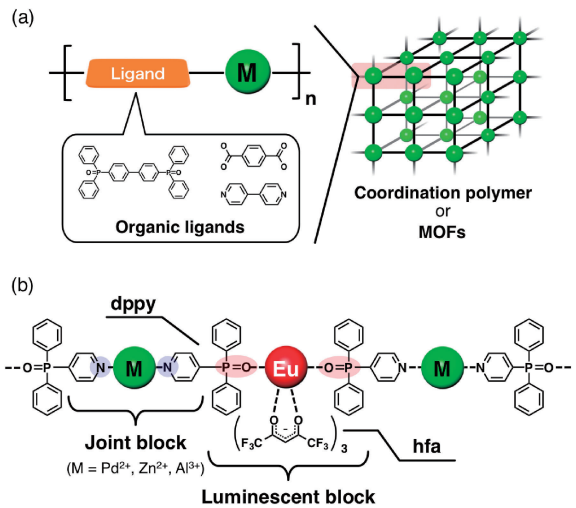

Figure 1. (a) General images of coordination polymers or MOFs. (b) Structural image of the Eu^{3+} complex ($M = Pd^{2+}$, Zn^{2+} and Al^{3+}).

1. Introduction

Three-dimensional building blocks composed of metal ions and organic bridged ligands are called "coordination polymers" or "metal-organic frameworks". Transition metal-organic frameworks (MOFs) with catalytic and ion-sensing properties have been reported.[1–3] Various types of metalloporphyrin aggregates such as coordination polymers for study of artificial photosynthesis have also been reported.[4,5] Thermostable luminescent coordination polymers with lanthanide ions have been presented for future photonic materials.[6,7] MOFs and metal coordination polymers with characteristic chemical and physical properties can be synthesized by suitable selection of metal ions and bridged organic ligands (Figure 1a).

Generally, three-dimensional structures of metal coordination polymers and MOFs are dominated by the coordination number and geometric structure of the metal ions. The coordination number and geometric structure in metal coordination polymers are directly linked to their chemical and physical performances for functional molecular materials. Here, we present luminescent coordination polymers composed of luminescent and joint metal blocks (Figure 1b). The structural and physical properties of these coordination polymers can be tuned by changing the composition of luminescent and joint metal blocks.

For the luminescent metal block, we selected lanthanide complexes with 4*f*-4*f* transitions. The 4*f*-4*f* transitions of lanthanide complexes lead to narrow emission bands (FWHM < 10 nm) and long emission lifetime ($\tau > 1\,\mu s$), resulting in the formation of remarkable luminescent materials for various applications such as display devices and bio-imaging applications.[8,9] Strong and characteristic luminescence of lanthanide complexes including Eu^{3+}, Tb^{3+}, Sm^{3+}, Nd^{3+}, Er^{3+}, Yb^{3+} and Pr^{3+} ions have been reported.[10–17] In earlier studies, the luminescent properties of lanthanide complexes were shown to depend on two parameters, radiative and non-radiative rate constants (k_r and k_{nr}).[18,19] The radiative rate constant depends on the

© 2018 The Chemical Society of Japan

geometric symmetry of the coordination structure in lanthanide complexes. It has been widely accepted that the radiative transition probability between 4*f* orbitals is enhanced by structures.[18] The non-radiative rate constant is influenced by the vibrational structures of lanthanide complexes. Previously, we prepared a Eu^{3+} complex with low-vibrational frequency (LVF) hexafluoroacetylacetonato (hfa) and phosphine oxide ligands. The coordination structure composed of LVF hfa (C-F: 1200 cm^{-1}) and phosphine oxide (P=O: 1125 cm^{-1}) ligands provides a luminescent Eu^{3+} complex with a high emission quantum yield (>65%) and a relatively small non-radiative rate constant.[20,21]

In order to construct joint metal blocks, we considered the use of *p*- and *d*-block metal complexes with various coordination structures. The *p*- and *d*-block metal complexes generally provide four, five and six coordination structures.[22–24] Based on the characteristic coordination structures of *p*- and *d*-block metal complexes, one-, two- and three-dimensional networks as a joint metal block are promoted for construction of novel coordination polymer. We here designed some joint metal blocks composed of metal ions and 4-pyridyldiphenylphosphine oxide (dppy). The dppy molecule in joint metal blocks possesses a phosphine oxide group, which plays an important role in effective connection with luminescent lanthanide blocks such as an LVF phosphine oxide. The pyridyl group in dppy is linked to the *p*- and *d*-block metal ions for formation of joint metal blocks. By using dppy molecules, Pd^{2+} complexes [*trans*-$PdCl_2(dppy)_2$], Zn^{2+} complexes [$ZnCl_2(dppy)_2$], and Al^{3+} complexes [$AlCl_3(dppy)_4$] were prepared as joint metal blocks.

In this study, we prepared $[Eu(hfa)_3(dppy)_2PdCl_2]_n$ (Eu-Pd), $[Eu(hfa)_3(dppy)_2ZnCl_2]_n$ (Eu-Zn), and $[Eu(hfa)_3(dppy)_4AlCl_3]_n$ (Eu-Al). According to the Eu-Zn polymer, we have already reported.[25] We here focus on the heavy element such as Pd^{2+} ions, and the light element, Al^{3+} ions, which have higher coordination number than that of Zn^{2+} ions. We report the effects on photophysical properties of these Eu^{3+} coordination polymers by using different metal ions. The predicted structures were estimated by single-crystal X-ray structural analyses and DFT calculations. Photophysical properties were evaluated based on the emission lifetimes and emission quantum yields. The preparation, structures and photophysical properties of new Eu^{3+} coordination polymers linked with joint metal blocks are described.

2. Experimental

Materials. 4-Bromopyridine hydrochloride (98%), tetrakis-(triphenylphosphine)palladium (97%), diphenylphosphine (90%) and hexafluoroacetylacetone (95%) was purchased from Tokyo Chemical Industry Co., Ltd. Europium(III) acetate n-hydrate (99.9%), palladium(II) chloride (98%), zinc(II) chloride (99.9%) and aluminum(III) chloride (99%) were obtained from Wako Pure Chemical Industries, Ltd. All other chemicals were reagent grade and were used without further purification.

Apparatus. ^{1}H NMR spectra were recorded on a JEOL JNM-ECS400 (400 MHz). ^{1}H NMR chemical shifts were determined with tetramethylsilane (TMS) as an internal standard. Elemental analyses were performed using a J-SCIENCE MICRO CORDER JM10. ESI-MS and FAB-MS were performed using a JEOL JMS-T100LP and a JEOL JMS-700TZ, respectively.

Preparation of 4-Pyridyl Diphenyl Phosphine Oxide (dppy) $C_{17}H_{14}NOP$. Dppy was prepared according to literature references.[25] ^{1}H NMR (400 MHz, $CDCl_3$/TMS): δ8.74–8.79 (t, 2H, py), 7.48–7.71 (m, 12H, Ar) ppm. ESI-MS calcd. for $[M + H]^+$: 280.09 Found, 280.09. Elemental analysis calcd (%) for $C_{17}H_{14}NOP$: C 73.11, H 5.05, N 5.02; found: C 73.03, H 5.07, N 4.95.

Preparation of Pd^{2+} Complex [*trans*-$PdCl_2(dppy)_2$]. Palladium(II) chloride (88.6 mg, 0.50 mmol) and 4-pyridyl diphenyl phosphine oxide (0.28 g, 1.00 mmol) were dissolved in toluene (40 mL). The solution was heated at 100 °C and refluxed while stirring for 48 h. The solvent was evaporated to afford a yellow powder. Recrystallization from methanol gave yellow crystals of the titled compound. (0.27 g, 72%) ^{1}H NMR (400 MHz, $CDCl_3$/TMS): δ8.92–8.97 (t, 4H, py), 7.49–7.68 (m, 24H, Ar) ppm. ESI-MS calcd. for $[M + Cl]^+$: 770.97 Found, 770.94. Elemental analysis calcd (%) for $C_{34}H_{28}Cl_2N_2O_8P_2Pd+CH_3OH$: C 54.74, H 4.20, N 3.65; found: C 54.62, H 3.84, N 3.77.

Preparation of Zn^{2+} Complex [$ZnCl_2(dppy)_2$]. [$ZnCl_2(dppy)_2$] was prepared according to literature references.[25] ^{1}H NMR (400 MHz, $CDCl_3$/TMS): δ = 8.84–8.89 (t, 4H, py), 7.71–7.77 (d, 4H, py), 7.62–7.70 (m, 12H, Ar), 7.50–7.57 (m, 8H, Ar) ppm. ESI-MS calcd. for $[ZnCl(dppy)_2]^-$: 692.03 Found, 692.03. Elemental analysis calcd (%) for $C_{34}H_{28}Cl_2N_2O_2P_2Zn$: C 58.77, H 4.06, N 4.03; found: C 59.27, H 4.31, N 3.73.

Preparation of Al^{3+} Complex [$AlCl_3(dppy)_4$]. Aluminum(III) chloride (74.4 mg, 0.56 mmol) and 4-pyridyl diphenyl phosphine oxide (0.50 g, 1.81 mmol) were dissolved in chloroform (40 mL). The solution was heated at 60 °C and refluxed while stirring for 24 h. The solvent was evaporated to afford a white powder of the titled compound. (91.0 mg, 13%) ^{1}H NMR (400 MHz, MeOD/TMS): δ8.84–8.89 (t, 8H, py), 7.89–7.96 (d, 8H, py), 7.68–7.76 (m, 24H, py), 7.58–7.65 (m, 16H, Ar) ppm. ESI-MS calcd. for $[AlCl_3(dppy)_4 \cdot 5H_2O + H]^+$: 1339.27 Found, 1339.16.

Preparation of Eu-Pd Complex $[Eu(hfa)_3(dppy)_2PdCl_2]_n$. Pd^{2+} complex [*trans*-$PdCl_2(dppy)_2$] (1 equiv.) and [$Eu(hfa)_3(H_2O)_2$] (1 equiv.) were dissolved in THF. The solution was refluxed while stirring for 5 h, and the reaction mixture was concentrated to dryness. A single crystal suitable for X-ray structural determination of Eu-Pd complex was obtained by diffusion of a methanol-chloroform solution at room temperature. FAB-MS calcd. for $[Eu(hfa)_3(dppy)PdCl_2]^+$: 1300.90 Found, 1300.9. Elemental analysis calcd (%) for $C_{49}H_{31}Cl_2EuF_{18}N_2O_8P_2Pd$: C 39.00, H 2.07, N 1.86, Cl 4.70; found: C 38.83, H 2.41, N 1.80, Cl 4.73.

Preparation of Eu-Zn Complex $[Eu(hfa)_3(dppy)_2ZnCl_2]_n$. $[Eu(hfa)_3(dppy)_2ZnCl_2]_n$ was prepared according to literature references.[25] FAB-MS calcd. for $[Eu(hfa)_3(dppy)ZnCl_2]^+$: 1258.93 Found, 1259.9. Elemental analysis calcd (%) for $C_{49}H_{31}Cl_2EuF_{18}N_2O_2P_2Zn+2H_2O$: C 39.13, H 2.35, N 1.86; found: C 38.73, H 2.25, N 1.88.

Preparation of Eu-Al Complex $[Eu(hfa)_3(dppy)_4AlCl_3]_n$. Al^{3+} complex [$AlCl_3(dppy)_4$] (1 equiv.) and [$Eu(hfa)_3(H_2O)_2$] (2 equiv.) were dissolved in methanol. The solution was refluxed while stirring for 5 h, and the reaction mixture was

© 2018 The Chemical Society of Japan

concentrated to dryness. ^{1}H NMR (400 MHz, $CDCl_3$/TMS): δ8.91–8.73 (br, 8H, py), 8.10–7.36 (br, 48H, Ar), 5.05 (s, 3H, hfa-H) ppm. FAB-MS calcd. for $[Eu(hfa)_2(dppy)_4AlCl_2]^+$: 1952.16 Found, 1952.5.

Computational Details. Density functional theory (DFT) geometry optimizations of joint Zn^{2+} block $[ZnCl_2(dppy)_2]$ and joint Al^{3+} block $[AlCl_3(dppy)_4]$ were carried out with Gaussian09 Rev D.01 by employing the three-parameter hybrid functional of Becke based on the correlation functional of Lee, Yang, and Parr (B3LYP).[26,27] The 6-31G(d) basis set was used for all other atoms.

Crystallography. Colorless single crystals of Eu^{3+} and Pd^{2+} complex were mounted on the MiTeGen micromesh using paraffin oil. All measurements were made by using a Rigaku RAXIS RAPID imaging-plate area detector with graphite-monochromated Mo-Kα radiation. Non-hydrogen atoms were refined anisotropically. All calculations were performed by using the crystal-structure crystallographic software package. CIF data was confirmed by using the checkCIF/PLATON service. CCDC-1507442 for $[Eu(hfa)_3(dppy)_2]$ and CCDC-1510581 for [*trans*-$PdCl_2(dppy)_2$] contain the supplementary crystallographic data for this paper. These data can be obtained free of charge from The Cambridge Crystallographic Data Centre via www.ccdc.cam.ac.uk/data_request/cif.

Optical Measurements. Emission and excitation spectra of Eu^{3+} complexes were measured with a HORIBA Fluorolog-3 spectrofluorometer and corrected for the response of the detector system. Emission lifetimes (τ_{obs}) of Eu^{3+} complexes were measured using the third harmonics (355 nm) of a Q-switched Nd:YAG laser (Spectra Physics, INDI-50, FWHM = 5 ns, λ = 1064 nm) and a photomultiplier (Hamamatsu photonics, R5108, response time ≤ 1.1 ns). The Nd:YAG laser response was monitored with a digital oscilloscope (Sony Tektronix, TDS3052, 500 MHz) synchronized to the single-pulse excitation. Emission lifetimes were determined from the slope of logarithmic plots of the decay profiles.

3. Results and Discussion

Network Structures. 4-pyridyldiphenylphosphine oxide (dppy) contains selective coordination sites for lanthanide ions (P=O) and metal ions (N atoms). The dppy was synthesized by the coupling reaction of 4-bromopyridine hydrochloride with diphenylphosphine and Pd^0 complex as a catalyst, and then oxidized using hydrogen peroxide. Joint metal blocks were prepared by the complexation of metal chlorides (palladium, zinc and aluminum chlorides) with dppy in an organic solvent under reflux conditions. Finally, $[Eu(hfa)_3(dppy)_2PdCl_2]_n$ (Eu-Pd), $[Eu(hfa)_3(dppy)_2ZnCl_2]_n$ (Eu-Zn) and $[Eu(hfa)_3(dppy)_4AlCl_3]_n$ (Eu-Al) were prepared by the complexation of $[Eu(hfa)_3(H_2O)_2]$ with a *p*- or *d*-metal joint block (Scheme 1). The chemical structures were confirmed by MS (ESI- and FAB-MS) and elemental analyses. Single crystals of $[Eu(hfa)_3(dppy)_2]$ and [*trans*-$PdCl_2(dppy)_2$] for X-ray structural analyses were successfully prepared by recrystallization from solutions in diethyl ether/hexane and methanol, respectively. However, single crystals of Eu-Zn and Eu-Al were not obtained. The structures of $[ZnCl_2(dppy)_2]$ and $[AlCl_3(dppy)_4]$ were estimated using DFT calculation (B3LYP/6-31G(d)) based on previous X-ray crystal data for a pyridyl metal complex derivative.[28,29]

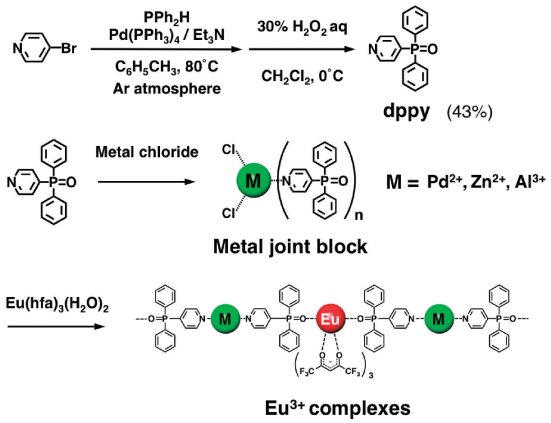

Scheme 1. Synthetic schemes of phosphine oxide ligand and Eu^{3+} complexes.

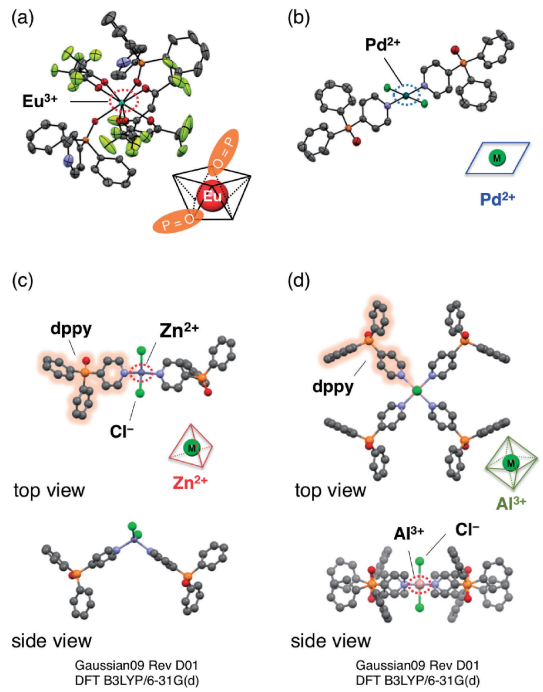

Figure 2. Structures of the luminescent Eu^{3+} block and joint metal blocks. ORTEP views of (a) luminescent Eu^{3+} block: $[Eu(hfa)_3(dppy)_2]$ and (b) joint Pd^{2+} block: [*trans*-$PdCl_2(dppy)_2$]. Hydrogen atoms have been omitted for clarity and thermal ellipsoids are shown at the 50% probability level. Structure optimizations of (c) joint Zn^{2+} block: $[ZnCl_2(dppy)_2]$ and (d) joint Al^{3+} block: $[AlCl_3(dppy)_4]$ using DFT calculations based on previous X-ray crystal data for a pyridyl metal complex derivative.[28,29]

Structural images and crystal data are shown in Figure 2 and Table S1, respectively. From the result of single-crystal X-ray diffraction, the coordination site of the luminescent Eu^{3+} block $[Eu(hfa)_3(dppy)_2]$ is comprised of three hexafluoroacetylacetonato (hfa) ligands and two phosphine oxide (dppy) ligands (Figure 2a). We carried out calculations of the shape measure factor *S* to estimate the degree of distortion of the coordination structure in the Eu^{3+} coordination sphere. The *S* value is given by eq (1):

© 2018 The Chemical Society of Japan

$$S = \min \sqrt{\left(\frac{1}{m}\right) \sum_{i=1}^{m} (\delta_i - \theta_i)^2}, \quad (1)$$

where m, δ_i, and θ_i are the number of possible edges ($m = 18$ in this study), the observed dihedral angle between planes along the i th edge, and the dihedral angle for the ideal structure, respectively. According to the crystals data of the luminescent Eu^{3+} block $[Eu(hfa)_3(dppy)_2]$, the S values for 8-SAP (point group D_{4d}, $S = 7.92$) are smaller than those for 8-TDH (point group D_{2d}, $S = 9.37$), suggesting that the 8-SAP structure is less distorted than the 8-TDH structure in the systems. Thus, the coordination geometry of the luminescent Eu^{3+} block $[Eu(hfa)_3(dppy)_2]$ was determined to be 8-SAP like structures (see Figure S1 and Table S2 in supporting information).

From the result of single-crystal X-ray diffraction, the coordination site of the joint Pd^{2+} block [*trans*-$PdCl_2(dppy)_2$] is composed of two chloride ions and two phosphine oxide ligands (Figure 2b). The Pd^{2+} complex shows four planar coordination structures without structural distortion, being similar to those of a previously reported Pd^{2+} complex.[30] From the structural analysis, we determined that the Pd complex formed trans-isomer.

Concerning the Zn^{2+} complex with pyridyl groups, Englert and co-workers have reported $[ZnCl_2(3,5\text{-}Me_2py)_2]$ (3,5-Me_2py: 3,5-dimethylpyridine) with tetrahedral structure.[28] We estimated the structure of our joint Zn^{2+} block using DFT calculation based on the previous X-ray single crystal data. The results of DFT calculation showed that the joint Zn^{2+} block was also composed of chloride ions and phosphine oxide ligands (Figure 2c). The coordination geometry of the joint Zn^{2+} block provides a tetrahedral structure.

Kemniz and co-workers have also described octahedral Al^{3+} complex $[AlBr_3(py)_4]$ (py: pyridine). They also reported that the bromide counter anion existed around Al^{3+} complex.[29] From these results, we assumed that the chloride counter anion existed around the joint Al^{3+} block. Thus, the structural optimization of the joint Al^{3+} block was evaluated by DFT calculation based on the $[AlCl_2(dppy)_4]^+$. The joint Al^{3+} block shows an octahedral structure with three chloride ions and four phosphine oxide ligands (Figure 2d).

We also consider that the joint Zn^{2+} block in Eu-Zn is a tetrahedral structure formed by two chloride ions and two phosphine oxide ligands, resulting in the formation of a one-dimensional Eu-Zn polymer structure. The ESI-MS fragment of Eu-Zn ($[Eu(hfa)_2(dppy)_2ZnCl_2]^+$) is similar to that of the one-dimensional structure of Eu-Pd ($[Eu(hfa)_2(dppy)_2ZnCl_2]^+$).

From these findings, we consider that Eu-Pd, Eu-Zn and Eu-Al complexes have a one-dimensional network structure.

Luminescence Properties. The emission spectra for Eu-Al and Eu-Pd complex in a solid state are shown in Figure 3a. Emission bands were observed at around 578, 592, 613, 650, and 698 nm, and they are attributed to 4*f*–4*f* transitions of Eu^{3+} ($^5D_0 \rightarrow {}^7F_J$: $J = 0$, 1, 2, 3, and 4), respectively. The spectra were normalized with respect to the magnetic dipole transition intensities (MD) at 592 nm ($^5D_0$–$^7F_1$), which are insensitive to the surrounding environment of the Eu^{3+} ions. The emission bands at around 613 nm are due to the electric dipole (ED) transitions, which are strongly dependent on the coordination geometry.[18] The spectral shapes of emission bands at around

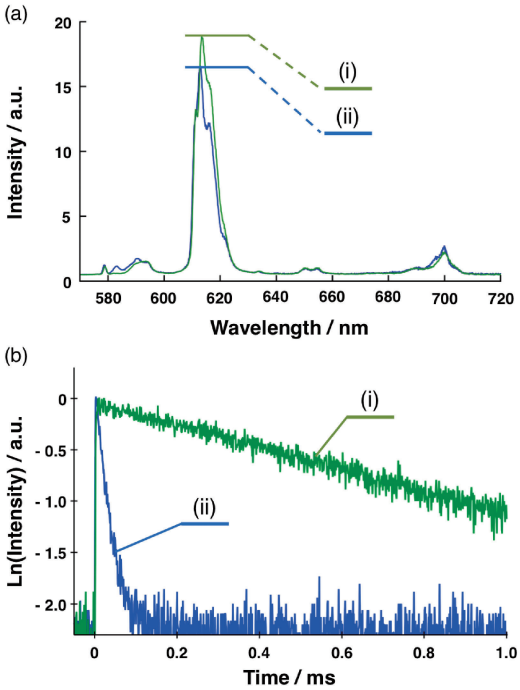

Figure 3. (a) Emission spectra of Eu^{3+} complexes (i) Eu-Al and (ii) Eu-Pd in solid state at room temperature excited at 350 nm. (b) Emission lifetime decays of Eu^{3+} complexes (i) Eu-Al and (ii) Eu-Pd in solid state at room temperature excited at 355 nm and detected at 610 nm (third harmonics of Q-switched Nd:YAG laser. FWHM = 5 ns, $\lambda = 1064$ nm).

613 nm of Eu-Al and Eu-Pd complex are related to their coordination geometry. The ED transition intensity of Eu-Al is larger than those of Eu-Pd. The large ED transition intensity is linked to the asymmetric structure of Eu-Al and enhanced k_r constant.

Emission lifetimes observed from the $^5D_0$ excited level (τ_{obs}) were determined from the slope of the logarithmic decay profiles (Figure 3b). The time-resolved emission profile of Eu-Al shows a single exponential decay with millisecond-scale lifetime. The emission lifetime for Eu-Al was determined to be 0.80 ms. In contrast, the time-resolved emission profile of Eu-Pd also shows a single exponential decay with microsecond-scale lifetime. The emission lifetime for Eu-Pd was determined to be 22 µs.

The values of k_r, k_{nr}, and Φ_{ff} were calculated using τ_{obs} and emission spectra by the following equations.[31,32]

$$\Phi_{ff} = \frac{k_r}{k_r + k_{nr}} = \frac{\tau_{obs}}{\tau_{rad}} \quad (2)$$

$$\frac{1}{\tau_{rad}} = A_{MD} n^3 \left(\frac{I_{tot}}{I_{MD}}\right) \quad (3)$$

$$k_r = \frac{1}{\tau_{rad}} \quad (4)$$

$$k_{nr} = \frac{1}{\tau_{obs}} - \frac{1}{\tau_{rad}}, \quad (5)$$

where A_{MD} is the spontaneous emission probability for $^5D_0 \rightarrow {}^7F_1$ transition in vacuo (14.65 s^{-1}), n is the refractive index of the medium (An average index of refraction equal to

© 2018 The Chemical Society of Japan

Table 1. Photophysical properties of Eu^{3+} complexes in the solid state

	Φ_{ff}[a]	$\Phi_{\pi\pi}$[b]	η_{sens}[c]	τ_{obs}[d]	k_r[e]	k_{nr}[f]
	%	%	%	μs	s^{-1}	s^{-1}
Eu-Al	72	52	72	800	9.0×10^2	3.5×10^2
Eu-Pd	1.3	—[g]	—	22	6.0×10^2	4.5×10^4
Eu-Zn[h]	59	28	48	850	7.0×10^2	4.8×10^2

[a] The intrinsic emission quantum yields were calculated from $\Phi_{ff} = k_r/(k_r + k_{nr}) = \tau_{obs}/\tau_{rad}$. [b] The total emission quantum yields Φ_{tot} were measured by integrating sphere (excitation at 370 nm). [c] The photo-sensitization efficiencies were calculated from $\eta_{sens} = \Phi_{tot}/\Phi_{ff}$. [d] Emission lifetime (τ_{obs}) of Eu^{3+} complexes were measured by excitation at 355 nm (Nd:YAG 3ω). [e] Radiative rate constants (k_r) for Eu^{3+} complexes estimated from $1/\tau_{rad} = A_{MD}n^3(I_{tot}/I_{MD})$.[31,32] [f] Non-radiative rate constant $k_{nr} = 1/\tau_{obs} - 1/\tau_{rad}$. [g] We could not observe. Emission was very weak. [h] Ref. 25.

1.5 was employed.),[33] and (I_{tot}/I_{MD}) is the ratio of the total area of the corrected Eu^{3+} emission spectrum to the area of the $^5D_0 \rightarrow {}^7F_1$ band. The photophysical properties of Eu^{3+} complexes linked with joint metal blocks are summarized in Table 1. The emission quantum yield of Eu-Al and Eu-Pd were estimated to be 72% and 1.3%, respectively. The Eu-Al complex shows a large emission quantum yield ($\Phi_{ff} = 72\%$), which is based on the large k_r and small k_{nr}. The large k_r of Eu-Al is most likely caused by the enhancement of the ED transition based on the asymmetric coordination geometry. In the previous study, we found that the radiative rate constant k_r of luminescent Eu^{3+} complexes was enhanced by the asymmetric coordination geometry with various types of phosphine ligands, and these Stark splittings in emission spectra are dependent on the steric structures of lanthanide complexes with phosphine ligands.[21] It should be noted that the coordination site of Eu^{3+} ions of Eu-Al, Eu-Zn, and Eu-Pd are similar structure, which are comprised of three hfa ligands and two dppy ligands. Thus, the radiative rate constants k_r of these Eu^{3+} complexes were expected to be similar value. We observed that k_r of Eu-Al is larger than that of Eu-Pd, although the Stark splitting shape of Eu-Al is similar to that of Eu-Pd (see Figure S2 in supporting information). From these photophysical findings, the large k_r of Eu-Al seems to be affected by not only the asymmetric coordination geometry but also electronic structure of joint Al^{3+} parts. The small k_{nr} of Eu-Al is probably caused by the rigid network structure. The emission quantum yield of Eu-Al is larger than those of Eu-Zn and Eu-Pd complex.

The Eu-Pd complex shows a much smaller emission quantum yield. We propose that both the characteristic emission lifetime profile and smaller quantum yield of Eu-Pd are caused by the excited quenching from the emitting level of Eu^{3+} ions. The weak emission spectrum of joint Pd^{2+} block [*trans*-$PdCl_2(dppy)_2$] at 88 K was observed at around 760 nm, which is attributed to MLCT transitions from the Pd^{2+} ion to phosphine oxide ligands (see Figure S3 in supporting information).[34] The energy transfer diagram of Eu^{3+} complex linked with Pd^{2+} complexes is shown in Figure 4. The energy level of MLCT of the Pd^{2+} complex is lower than that of the excited $^5D_0$ state of Eu^{3+} ions. The small emission quantum yield of the Eu-Pd

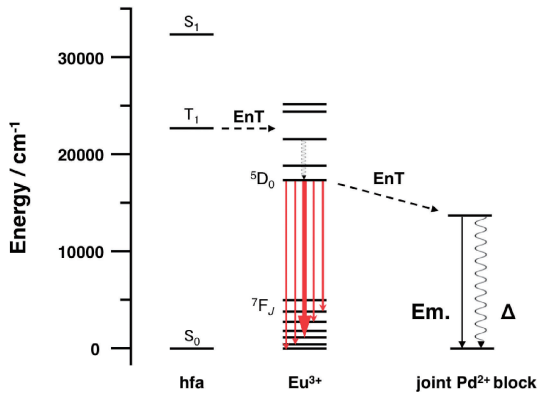

Figure 4. Energy diagram of Eu^{3+} complexes linked with joint Pd^{2+} blocks (EnT: energy transfer).

complex is caused by the energy transfer from luminescent Eu^{3+} blocks to joint Pd^{2+} blocks.

It is well known that the radiative and non-radiative rate constants of a lanthanide complex are dependent on the organic ligand or the solvent molecules.[35] In this study, all of the Eu^{3+} coordination sites in Eu^{3+} complexes were attached to three hfa and two dppy ligands. The photophysical properties of the Eu^{3+} complexes could be linked to moieties of metal ions (steric and electronic properties) in the joint metal blocks.

We also calculated the photo-sensitized energy transfer efficiency, η_{sens} based on the Φ_{ff} and $\Phi_{\pi\pi^*}$. In Table 1, η_{sens} of Eu-Al ($\eta_{sens} = 72\%$) is much larger than those of Eu-Zn ($\eta_{sens} = 48\%$). The η_{sens} of Eu-Al is also much larger from that of previous $[Eu(hfa)_3(dpbp)_2]_n$ ($\eta_{sens} = 40\%$).[36] We consider that the polymeric structure effect from rigid zig-zag structure led to enhanced η_{sens}.[37]

4. Conclusion

We have synthesized Eu^{3+} complex composed of luminescent Eu^{3+} and joint Al^{3+} and *trans*-Pd^{2+} complexes. The structures and photophysical properties of these Eu^{3+} complexes are dependent on the joint metal blocks. The emission quantum yield of the Eu-Al complex is the largest in these Eu^{3+} complex linked with joint metal blocks.

We consider that the network structure of the Eu-Al complex based on the coordination structure of joint Al^{3+} blocks leads to a large radiative rate constant and small non-radiative rate constant, resulting in a high emission quantum yield ($\Phi_{ff} = 72\%$). The high triplet energy level of joint metal blocks such as Al^{3+} ions might promote effective luminescence. In contrast, the emission quantum yields of Eu-Pd was found to be 1.3%. The small emission quantum yield of the Eu-Pd complex is caused by the energy transfer from luminescent Eu^{3+} ions to joint Pd^{2+} complexes. In this study, we provide a new design of Eu^{3+} complex linked with joint metal blocks for control of geometric structure and photophysical properties.

This work was supported by a Grant-in-Aid for Scientific Research on Innovative Area of "New Polymeric Materials Based on Element-Blocks" from the Ministry of Education, Culture, Sports, Science and Technology (MEXT), Japan (grant number 2401). This present research was supported by the Ministry of Education, Culture, Sports, Science and Technol-

© 2018 The Chemical Society of Japan

ogy through Program for Leading Graduate Schools (Hokkaido University "Ambitious Leader's Program").

Supporting Information

An additional experimental results including single-crystal X-ray structure analyses, shape-measure calculations, emission spectra, and diffuse reflection spectra. This material is available on http://dx.doi.org/10.1246/bcsj.20170241.

References

1 H.-J. Son, S. Jin, S. Patwardhan, S. J. Wezenberg, N. C. Jeong, M. So, C. E. Wilmer, A. A. Sarjeant, G. C. Schatz, R. Q. Snurr, O. K. Farha, G. P. Wiederrecht, J. T. Hupp, *J. Am. Chem. Soc.* **2013**, *135*, 862.

2 T. Zhang, W. Lin, *Chem. Soc. Rev.* **2014**, *43*, 5982.

3 J. Lee, O. K. Farha, J. Roberts, K. A. Scheidt, S. T. Nguyen, J. T. Hupp, *Chem. Soc. Rev.* **2009**, *38*, 1450.

4 B. Chen, L. Wang, F. Zapata, G. Qian, E. B. Lobkovsky, *J. Am. Chem. Soc.* **2008**, *130*, 6718.

5 J. Heine, K. Müller-Buschbaum, *Chem. Soc. Rev.* **2013**, *42*, 9232.

6 H. Zhang, L. Zhou, J. Wei, Z. Li, P. Lin, S. Du, *J. Mater. Chem.* **2012**, *22*, 21210.

7 K. Miyata, Y. Konno, T. Nakanishi, A. Kobayashi, M. Kato, K. Fushimi, Y. Hasegawa, *Angew. Chem., Int. Ed.* **2013**, *52*, 6413.

8 G. Shao, H. Yu, N. Zhang, Y. He, K. Feng, X. Yang, R. Cao, M. Gong, *Phys. Chem. Chem. Phys.* **2014**, *16*, 695.

9 S. J. Butler, L. Lamarque, R. Pal, D. Parker, *Chem. Sci.* **2014**, *5*, 1750.

10 N. M. Shavaleev, S. V. Eliseeva, R. Scopelliti, J.-C. G. Bünzli, *Chem.—Eur. J.* **2009**, *15*, 10790.

11 W.-S. Lo, J. Zhang, W.-T. Wong, G.-L. Law, *Inorg. Chem.* **2015**, *54*, 3725.

12 O. A. Blackburn, N. F. Chilton, K. Keller, C. E. Tait, W. K. Myers, E. J. Mclnnes, A. M. Kenwright, P. D. Beer, C. R. Timmel, S. Faulkner, *Angew. Chem., Int. Ed.* **2015**, *127*, 10933.

13 L. J. Daumann, D. S. Tatum, B. E. R. Snyder, C. Ni, G. Law, E. I. Solomon, K. N. Reymond, *J. Am. Chem. Soc.* **2015**, *137*, 2816.

14 M. M. Nolasco, P. M. Vaz, V. T. Freitas, P. P. Lima, P. S. André, R. A. S. Ferreira, P. D. Vaz, P. Ribeiro-Claro, L. D. Carlos, *J. Mater. Chem. A* **2013**, *1*, 7339.

15 V. Haquin, M. Etienne, C. Daiguebonne, S. Freslon, G. Calvez, K. Bernot, L. L. Pollès, S. E. Ashbrook, M. R. Mitchell, J.-C. Bünzli, S. V. Eliseeva, O. Guillou, *Eur. J. Inorg. Chem.* **2013**, 3464.

16 L. Song, J. Wang, J. Hu, X. Liu, Z. Zhen, *J. Alloys Compd.* **2009**, *473*, 201.

17 A. Ishii, S. Kishi, H. Ohtsu, T. Iimori, T. Nakabayashi, N. Ohta, N. Tamai, M. Melnik, M. Hasegawa, Y. Shigesato, *ChemPhysChem* **2007**, *8*, 1345.

18 Y. Hasegawa, Y. Wada, S. Yanagida, *J. Photochem. Photobiol., C* **2004**, *5*, 183.

19 A. F. Kirby, F. S. Richardson, *J. Phys. Chem.* **1983**, *87*, 2544.

20 K. Nakamura, Y. Hasegawa, H. Kawai, N. Yasuda, N. Kanehisa, Y. Kai, T. Nagamura, S. Yanagida, Y. Wada, *J. Phys. Chem. A* **2007**, *111*, 3029.

21 K. Miyata, T. Nakagawa, R. Kawakami, Y. Kita, K. Sugimoto, T. Nakashima, T. Harada, T. Kawai, Y. Hasegawa, *Chem.—Eur. J.* **2011**, *17*, 521.

22 J. Ni, Y.-G. Wang, H.-H. Wang, L. Xu, Y.-Q. Zhao, Y.-Z. Pan, J.-J. Zhang, *Dalton Trans.* **2014**, *43*, 352.

23 A. Rana, P. K. Panda, *Chem. Commun.* **2015**, *51*, 12239.

24 M. Sjödin, J. Gätjens, L. C. Tabares, P. Thuéry, V. L. Pecoraro, S. Un, *Inorg. Chem.* **2008**, *47*, 2897.

25 M. Yamamoto, T. Nakanishi, Y. Kitagawa, K. Fushimi, Y. Hasegwa, *Mater. Lett.* **2016**, *167*, 183.

26 C. Lee, W. Yang, R. G. Parr, *Phys. Rev. B* **1988**, *37*, 785.

27 A. D. Becke, *J. Chem. Phys.* **1993**, *98*, 5648.

28 C. Hu, U. Englert, *CrystEngComm* **2002**, *4*, 20.

29 A. Dimitrov, D. Heidemann, K. I. Khallow, E. Kemnitz, *Inorg. Chem.* **2012**, *51*, 11612.

30 G. Dahm, E. Borré, C. Fu, S. Bellemin-Laponnaz, M. Mauro, *Chem.—Asian J.* **2015**, *10*, 2368.

31 L. Prodi, M. Maestri, R. Ziessel, V. Balzani, *Inorg. Chem.* **1991**, *30*, 3798.

32 M. H. V. Werts, R. T. F. Jukes, J. W. Verhoeven, *Phys. Chem. Chem. Phys.* **2002**, *4*, 1542.

33 R. Pavithran, N. S. Saleesh Kumar, S. Biju, M. L. P. Reddy, S. A. Junior, R. O. Freire, *Inorg. Chem.* **2006**, *45*, 2184.

34 A. Krogul, J. Cedrowski, K. Wiktorska, W. P. Ozimiński, J. Skupińska, G. Litwinienko, *Dalton Trans.* **2012**, *41*, 658.

35 M. Morikawa, S. Tsunofuri, N. Kimizuka, *Langmuir* **2013**, *29*, 12930.

36 K. Miyata, T. Ohba, A. Kobayashi, M. Kato, T. Nakanishi, K. Fushimi, Y. Hasegawa, *ChemPlusChem* **2012**, *77*, 277.

37 Y. Hirai, T. Nakanishi, Y. Kitagawa, K. Fushimi, T. Seki, H. Ito, Y. Hasegawa, *Angew. Chem., Int. Ed.* **2016**, *55*, 12059.

© 2018 The Chemical Society of Japan